Developmental Neuroscience

Research Article

Dev Neurosci
DOI: 10.1159/000515197

Received: January 3, 2021
Accepted: February 11, 2021
Published online: April 13, 2021

Aluminum Microcomb Electrodes on Silicon Wafer for Detecting Val66Met Polymorphism in Brain-Derived Neurotrophic Factor

Zhi Li[a, b, c, d] Liangmin Cui[e] Hongyao Zhao[f] Jinxin Du[g]
Subash C.B. Gopinath[h, i] Thangavel Lakshmipriya[i] Xuezhi Xin[a, b, c, d]

[a]Department of General Surgery, The First Affiliated Hospital of Shandong First Medical University & Shandong Provincial Qianfoshan Hospital, Jinan, China; [b]Key Laboratory of Metabolism and Gastrointestinal Tumor, the First Affiliated Hospital of Shandong First Medical University, Jinan, China; [c]Key Laboratory of Laparoscopic Technology, the First Affiliated Hospital of Shandong First Medical University, Jinan, China; [d]Shandong Medicine and Health Key Laboratory of General Surgery, Jinan, China; [e]Department of Anorectal, The Second People's Hospital of Dongying, Jinan, China; [f]Department of Special Inspection, the First Affiliated Hospital of Shandong First Medical University, Jinan, China; [g]Department of Anorectal, Shandong university of traditional chinese medicine, Jinan, China; [h]Faculty of Chemical Engineering Technology, Universiti Malaysia Perlis, Arau, Malaysia; [i]Institute of Nano Electronic Engineering, Universiti Malaysia Perlis, Kangar, Malaysia

Keywords
Electrochemical sensor · Neurological disorder · Sandwich assay · Reporter DNA · DNA sensor

Abstract
Objective: Brain-derived neurotrophic factor (BDNF) dysregulation is widely related with various psychiatric and neurological disorders, including schizophrenia, depression, Rett syndrome, and addiction, and the available evidence suggests that BDNF is also highly correlated with Parkinson's and Alzheimer's diseases. ***Methods:*** The BDNF target sequence was detected on a capture probe attached on aluminum microcomb electrodes on the silicon wafer surface. A capture-target-reporter sandwich-type assay was performed to enhance the detection of the BDNF target. ***Results:*** The limit of detection was noticed to be 100 aM. Input of a reporter sequence at concentrations >10 aM improved the detection of the target sequence by enhancing changes in the generated currents. Control experiments with noncomplementary and single- and triple-mismatches of target and reporter sequences did not elicit changes in current levels, indicating the selective detection of the BDNF gene sequence. ***Conclusion:*** The above detection strategy will be useful for the detection and quantification of BDNF, thereby aiding in the provision of suitable treatments for BDNF-related disorders.

Introduction

Brain-derived neurotrophic factor (BDNF) plays an important role in neuronal survival and growth, serves as a neurotransmitter modulator, and participates in neuronal plasticity, which is essential for learning and memory. It is widely expressed in the CNS, gut and other tissues.

karger@karger.com
www.karger.com/dne

Correspondence to:
Xuezhi Xin, sinxz@sina.com

BDNF is a trophic factor regulating cell survival and synaptic plasticity, may play a critical role in gut motility. BDNF is expressed primarily in the central nervous system, but its expression is also detected in peripheral tissues such as the vascular endothelium and visceral epithelium, as well as in immune cells. BDNF plays a major role in neuronal function, plasticity, and modulation [1, 2], and its expression in the central nervous system is highly related to different biological functions such as cholinergic activity, synaptogenesis, N-methyl-D-aspartate receptor activity, and dendritogenesis [3, 4]. BDNF is critical for neuronal development and plasticity, and its dysregulation is associated with several psychiatric and neurological disorders, including depression, Rett syndrome, and schizophrenia [5]. Moreover, the decrement of BDNF has been observed in other neurological disorders, such as multiple sclerosis and Alzheimer's, Parkinson's, and Huntington's diseases [6]. Furthermore, BDNF expressions help predict the endometriosis presence [7]. BDNF expression was noticed to be 2-fold higher in endometriosis patients than in controls, while decreasing in patients with depressive disorders [8, 9].

BDNF gene encodes human chromosome 11p13, which exhibits as alternatively spliced upstream untranslated exons and a downstream exon IX exhibiting the common coding region and 3′ UTR. Interestingly, G>A nucleotide substitution at position 196 encodes a Val66Met substitution on the amino acid. Val66Met polymorphism has implicated differentially in the individual brain structure of the prefrontal cortex and function of the hippocampus, which are experience-dependent plasticity in the motor cortex, memory performance, and are related to reasoning skills. Since Val66Met polymorphism affects the brain structural network vulnerability, it is highly correlated with emotional and cognitive dysfunction by changing white matter structure and cerebral cortex excitability. It is responsible for various disorders, such as Parkinson's disease, neurocognitive dysfunction and childhood mood disorder, geriatric depression, and schizophrenia. Moreover, BDNF Val66Met polymorphism is related to the activity of glutamate receptors, which then changes the hippocampal long-term depression and anxiety-related disorder [10–12]. Therefore, the ability to accurately quantify the presence of BDNF is necessary for improved diagnosis of various diseases. Circulating BDNF amount was used to measure in serum, plasma, or whole blood. Under normal physiological conditions, the expression of BDNF varies depending on age, gender, and physical condition. In healthy human volunteers, the mean serum BDNF concentrations were measured at 32.69 ± 8.33 ng/mL; however, identifying BDNF concentrations below this concentration is necessary to predict the presence of various diseases, including brain disorders [13, 14]. This research work is aimed to develop a method of detection of Val66Met polymorphism of the BDNF gene by utilizing interdigitated electrode (IDE) electrochemical sensors.

Biosensing methods have been employed to diagnose various diseases using appropriate biomarkers, and several biosensors can detect diseases at earlier stages [15–18]. Among these, dielectric sensors can be effectively used to detect a range of diseases by transducing biological interactions into electrical signals [19–22]. These sensors use electrodes to detect the changes in electrical currents generated by biomolecular interactions with sensing surfaces. The resulting changes are considered to reflect the interaction and affinity of biomolecules. The system is simple, easy, and compact, and the sensing signal is obtained through the conducting element. Voltammetry is one of the commonly used and efficient dielectric strategies employed to detect various targets, including viruses, bacteria, heavy metals, DNA, RNA, proteins, and antibodies [23–26]. In this study, we used a dielectric sensor to detect a BDNF DNA target sequence through complementary binding to its capture probe.

DNA biosensors use DNA sequences as the biomolecular recognition tool to identify specific interactions between probes and target DNA and are usually detected through optical, thermal, or electrical transduction mechanisms [27, 28]. Electrical DNA sensors are particularly useful due to their higher sensitivity and capacity for faster diagnosis. A combination of DNA with a dielectric system allows for the determination of a broad range of targets, including bacteria, viruses, and various cancers, and helps to identify DNA damage [29–35]. In this study, BDNF was detected on a dielectric sensing surface using a BDNF sequence-specific capture probe. Moreover, to improve detection, a reporter sequence was utilized to determine the target utilizing a sandwich-like assay [12]. The sandwich strategy employing capture-target-reporter sequences was performed on the dielectric sensing surface to quantify Val66Met polymorphism of the BDNF gene.

Materials and Methods

Reagents

Streptavidin, PBS (pH 7.4), and 1,1′-carbonyldiimidazole (CDI) were bought from Sigma-Aldrich (St. Louis, MO, USA). Ethanolamine was obtained from Fisher Scientific (Loughbor-

ough, UK). BDNF DNA sequences were acquired as previously stated [12]. The biotinylated capture probe, target, reporter, and single- and triple-mismatched controls were synthesized by a local supplier. The sequences for the reverse strand of the *Homo sapiens* BDNF gene were obtained from GenBank (Accession No. AF411339.1). The following sequences were used: BDNF-Target (90-mer), 5′-ttggctgacactttcgaacacgtgatagaagagctgttggatgaggaccagaaagttcggcccaatgaagaaaacaataag gacgcagac-3′; BDNF-Capture (25-mer), 5′-biotin – AGTCTGCGTCCTTATTGTTTTCTTC-3′; and BDNF-Reporter (24-mer), 5′-AACCGACTGT GAAAGCTT-GTGCAC-3′.

Fabrication of IDE Sensor Surface

Aluminum microcomb electrode on a silicon wafer to form an IDE was prepared as described, with some physical modifications on the top of the sensing surface. Initially, the mask and basic design were made using the AutoCAD software. The desired dimensions are length, 7,500 μm; width, 4,000 μm; finger-gap pairs, 40; gap size, 1 μm; electrode size, 50 μm; and substrate thickness, 0.2 mm. For the fabrication process, initially, the electrodes with the similar size and number were designed by the software AutoCAD, and then with the photomask, the designed electrode was printed. The printed photomask was aligned on the surface of the glass to transfer the pattern. To fabricate the IDE surface, initially, the IDE silicon wafer (Si) base was cleaned with the solutions, RCA2 and RCA1, to remove the foreign substance from the surface and then oxidized by using aluminum (Al) coils under wet thermal oxidation for 1 h at 500°C. On the Al substrates, a positive photoresist was coated by using the spin coater and then backed for 1 min at 90° to eliminate the stationary wave and moisture on the IDE surface. The designed electrode was transferred to IDE by using the UV light for 10 s. And, then the surface was immersed in the photoresist developer to eliminate the unexposed area. After that, the electrode was backed at 110° (1 min) to strengthen the adhesion layer between Al and SiO_2 and to clear the moisture. Finally, the etching process was carried out by dipping the surface in Al etchant solution, and the fabricated device was washed with acetone followed by distilled water [36, 37].

Capture Probe Immobilization on the IDE Surface

A biotin-streptavidin conjugation pattern was conducted to attach the capture probe to the IDE. The surface was first CDI modified by placing diluted CDI (0.5 M, 100 μL) on the electrode (1 h) at room temperature. Excess CDI was removed from the surface using PBS (10 mM; pH 7.4). Then, tetravalent streptavidin (250 nM) was placed on the CDI-modified electrode (1 h) at room temperature. After washing, the CDI-modified electrode was masked with ethanolamine (1 M) for 1 h, following which 1 μM of the biotinylated capture probe was allowed to bind to the streptavidin-modified IDE surface. Between each functionalization step, the electrode was washed several times with buffer to prevent biofouling. Changes in the current level were recorded for each step to confirm binding.

Interaction of Target-Capture DNA Sequences with the IDE

The BDNF gene target was detected by the capture probe modified on the IDE. For that, 1 pM of target DNA (10 μL) was interacted with the immobilized probe for 30 min to permit binding. The electrode was then washed with 10 volumes of PBS to eliminate the unbound target, and the changes of current were compared. To test the limit of detection (LOD), different concentrations of the target sequence (10-fold serial dilutions, from 1 aM until 1 pM) were reacted (10 μL) individually with the capture on the modified IDE sensing electrode. Before and after base-pairing, changes in the generated currents were recorded to identify capture/target interactions. The surface was washed thoroughly before each reading to avoid nonspecific base-pairing.

Sandwich Assay for Capture-Target-Reporter on the IDE

Sandwich assays with capture-target-reporter DNA sequences were performed on the capture immobilized on the IDE to improve BDNF gene detection. For this assay, 1 μM of capture (10 μL) was first placed onto the surface as stated above, followed by 10 fM of target DNA (10 μL), and finally different dilutions (10 aM to 1 pM) of reporter sequence DNA (10 μL) were individually added. Changes in current were recorded before and after immobilization.

Selective and Specific Detection of BDNF Gene Sequence Base-Pairing

After quantification of the BDNF gene sequence expression, to confirm the selective detection on capture probe-modified surfaces, 3 different control experiments were performed using noncomplementary and single- and triple-mismatched target sequences. Each control sequence was independently dropped from the capture with the modified electrodes, and alterations in current were recorded and compared with those obtained with the correct target sequences. Moreover, to check the specific detection of the BDNF target gene, targets were spiked in undiluted human serum or human serum albumin (HSA) at 670 μM (45 mg/mL) (10 μL) and placed on the capture-modified electrodes for the comparative analysis with the current level.

Results and Discussion

This study focused on the detection of the BDNF gene sequence on the IDE sensing surface through the use of a suitable sequence-specific capture probe. For that, SNP rs6265 of the BDNF gene (GenBank Accession No. AF411339) at position 95422 was desired. The sequence for the reverse strand of the *Homo sapiens* BDNF gene was obtained from GenBank (Accession No. AF411339.1). The structure of the BDNF protein has been well characterized (PDB accession codes: 1B8K and 1B98) (Fig. 1a, b) [46]. Figure 1c displays the schematic for the determination of BDNF DNA using the IDE sensor. First, streptavidin was attached to the CDI-modified sensing surface, followed by attachment of the biotinylated capture probe and detection of the target sequence by base-pairing with the capture probe. To improve target DNA detection, the immobilized target was sandwiched using the reporter oligo.

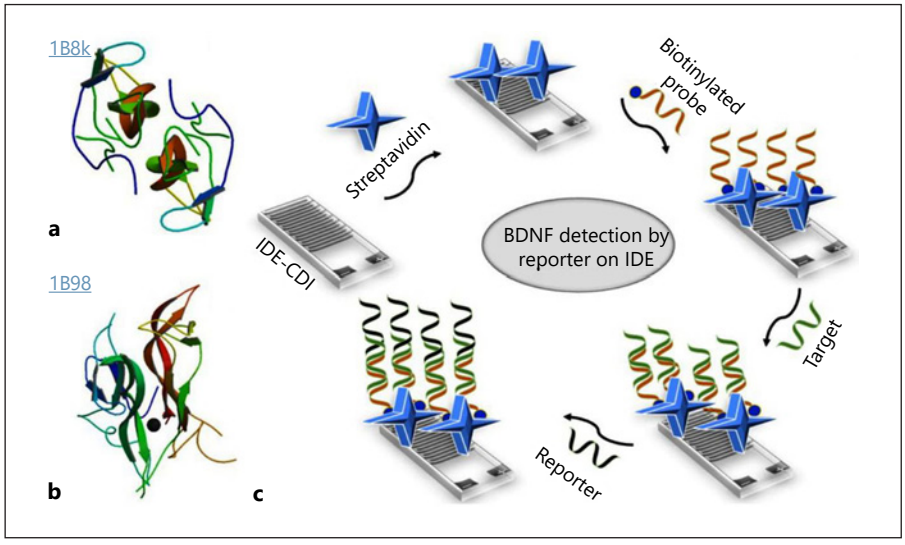

Fig. 1. Human neurotrophin-3 (**a**) and neurotrophin-4 (homodimer) (**b**) [46]. **c** Schematic representation of detection of the BDNF gene target sequence on the CDI-modified dielectrode sensing surface. The capture probe was immobilized on the IDE surface using a biotin-streptavidin strategy and detected through the target sequence. A capture-target-reporter sandwich assay was also carried out for improved detection of the BDNF gene. BDNF, brain-derived neurotrophic factor; CDI, carbonyldiimidazole; IDE, interdigitated electrode.

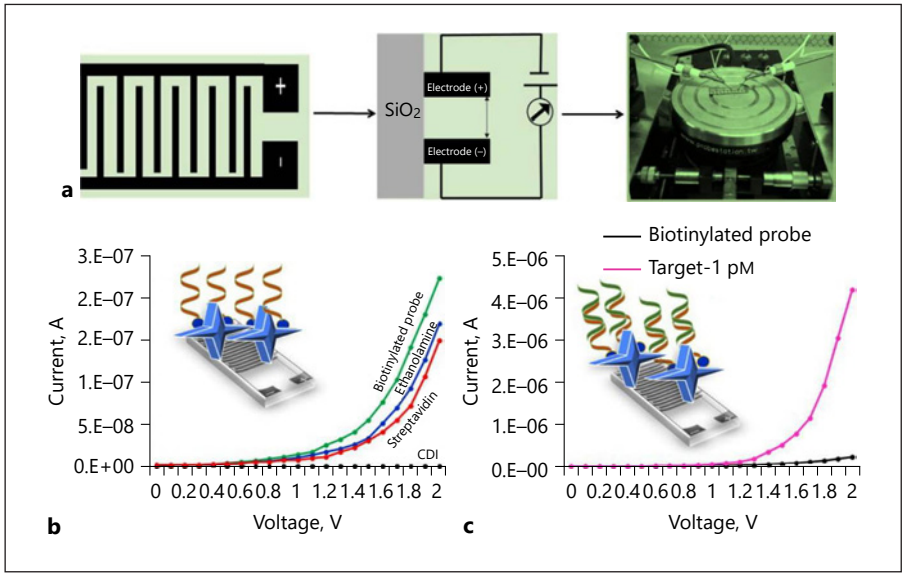

Fig. 2. a Measurement setup and the contact. The IDE pattern and the connecting system are shown. **b** Changes in current generated in the capture probe immobilization process on the IDE. Initially, CDI was dropped onto the sensing surface, followed by the addition of streptavidin. Then, the biotinylated capture probe was allowed to interact with streptavidin. The increased current level after each immobilization step was indicative of binding. **c** Target (1 pM) base-pairing with the immobilized capture probe. After adding the target DNA, the current generated was greatly increased. **Inset** A diagrammatic representation. CDI, carbonyldiimidazole; IDE, interdigitated electrode.

Surface Immobilization of the Capture Probe on the IDE Sensing Electrode

The measurement setup and the contact followed by the IDE are displayed in Figure 2a. A biotin-streptavidin conjugation strategy was utilized to attach the capture probe to the IDE. Current changes confirm the attachment of the capture probe to the surface (Fig. 2b). The CDI-modified IDE sensing surface displays a current of 1.58E–08 A. CDI is a well-known neutral coupling agent with affinity adsorbent properties, in which alkyl carbamate linkages are created between the hydroxylic support and an amine-containing ligand. CDI-functionalized surfaces exhibit imidazole carbamate functionality, producing a stable carbamate linkage with an amine group. CDI is commonly utilized to immobilize proteins or antibodies on sensing surfaces [38, 39]. In this study, streptavidin was placed on the CDI-modified surface, inducing a current level increment to 1.48E–07 A, clearly indicating the binding of streptavidin to the biotinylated probe on the surface. After streptavidin, the remaining CDI-modified surface was blocked with ethanolamine, resulting in a current change of 1.68E–07 A. The recorded change in current with the addition of ethanolamine is marginal due to the increased occupation of the CDI-modified surface by streptavidin. Finally, the biotinylated capture probe was added to the streptavidin surface, and

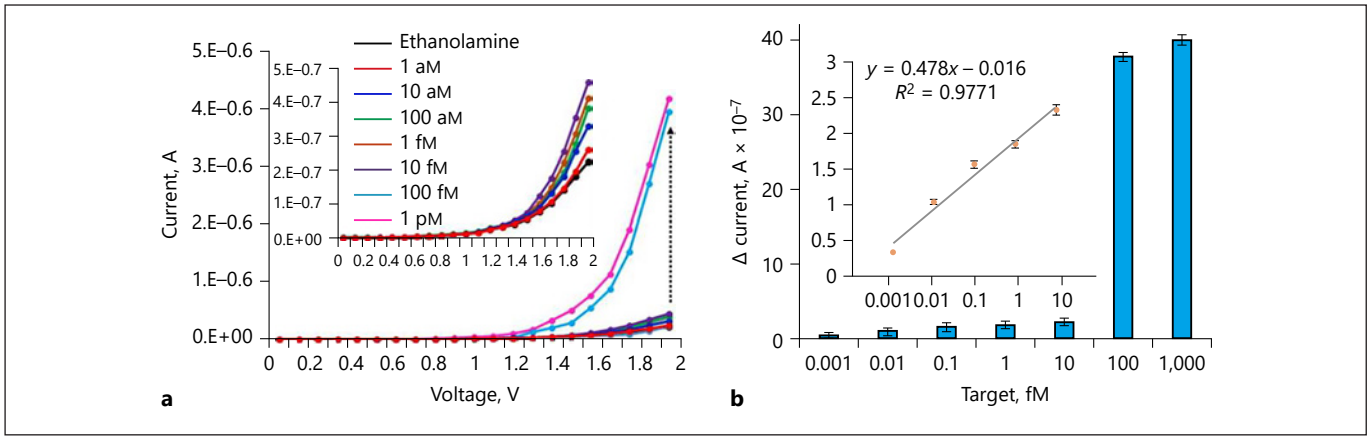

Fig. 3. a LOD of the BDNF gene target sequence. Target concentrations ranging from 1 aM to 1 pM were interacted with the surface-immobilized capture probes, and the changes in current were recorded. The current levels increased with increasing target concentrations. **b** Differences in current changes with target DNA binding to the capture probe. Target binding to the capture probe was saturated from 100 fm, and a linear regression line shows the LOD of the target to be 100 aM. Current measurements (**a**) were performed using Keithley 6487 with a linear sweep 0–2 V at the step of 0.1 V. LOD, limit of detection; BDNF, brain-derived neurotrophic factor.

the current level further increased to 2.22E−07 A. As streptavidin has 4 binding sites, a greater number of biotin molecules can bind to a single streptavidin molecule, increasing the capture probe binding capacity on the IDE sensing surface [40]. The sensitivity is highly dependent on the amount of capture probe attached to the sensing surface, with increased levels of base-pairing being expected to lead to an increase in the target detection signal [41, 42]. Here, an increased concentration of capture probes immobilized on the IDE surface was expected to improve the detection of the target BDNF gene sequence. Overall, the changes in the levels of current generated at each immobilization step confirmed that the surface preparation with the capture probe is suitable for the detection of the BDNF target.

Detection of the BDNF Gene Target on the IDE Surface

In general, researchers are choosing aluminum as a sensing substrate due to its easier availability and low cost. To overcome the influence of the oxidation of aluminum, an earlier study has evaluated the IDE surface with pH scouting, and a range of pH near neutral does not affect the detection of the surface charge. Due to this reason, PBS has been used in this study with pH 7.4. The BDNF target was detected by the capture probe immobilized on the IDE surface. When a high concentration (1 pM) of target DNA interacted with the capture probe on the surface, the current enhanced markedly from 2.2E−07 to 4.54E−06 A (Fig. 2c). This is an approximately 20-fold enhancement in the amount of current generated, which resulted from the base-pairing of the capture probe and target oligos. This result indicates the apparent detection of 1 pM of the BDNF gene target sequence. Usually, single-stranded DNA has a phosphate backbone and represents a more negative charge. When the target forms base-pairing, the phosphate backbone is masked, and there is a reduction in the negative charge, which gives a low response.

LOD of BDNF Target Genes on the IDE

To find the LOD, the target oligo concentration was diluted (1 pM to 1 aM) and independently dropped onto the capture probe-modified IDE, and the changes in current resulting from the base-pairing of the capture probe and target were recorded. As displayed in Figure 3a, when the concentration of the target DNA enhanced, the current generated also increased. The 1 aM concentration did not elicit a clear alter in the current; however, from 10 aM, changes in current became apparent. A 10 aM concentration of target DNA elicited the smallest change in current, from 2.2E−07 to 3.26E−07 A. At the 100 aM, 1 fM, 10 fM, 100 fM, and 1 pM concentration, the current levels were 3.78E−07, 4.06E−07, 4.54E−07, 4E−06, and 4.22E−06 A, respectively. At the 100 fM and 1 pM target concentrations, base-pairing saturation was achieved. These results indicate a clear interaction between the capture probe and target on the IDE surface. Figure 3b shows the profile

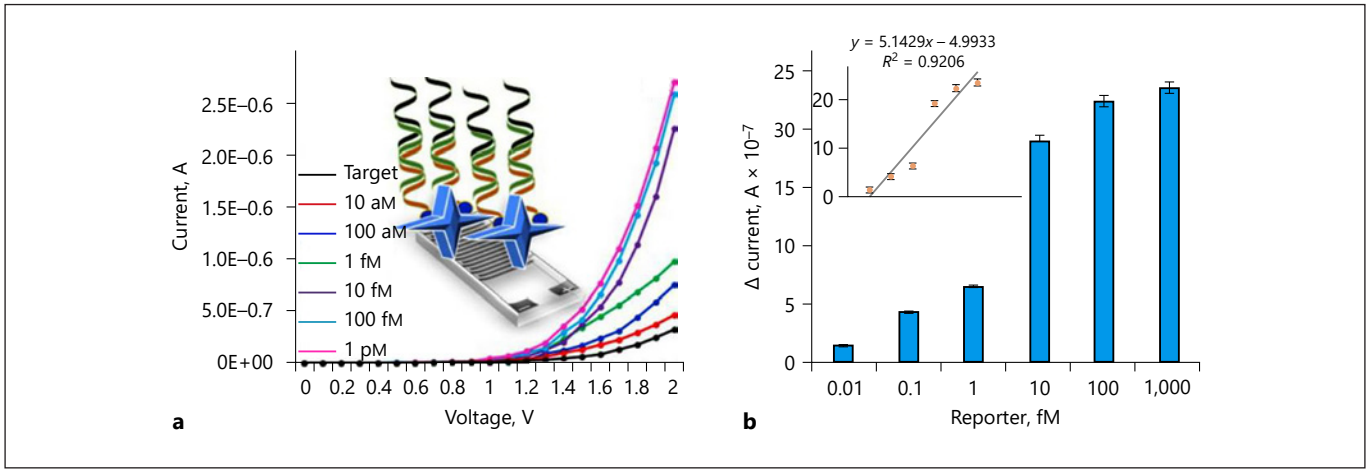

Color version available online

Fig. 4. a Capture-target-reporter sandwich assay was carried out on the IDE surface. Capture probe (1 M) was allowed to interact with 10 aM of the target DNA and detected by different reporter concentrations (10 aM to 1 pM). The current levels were also increased with increasing reporter concentrations. **Inset** A diagrammatic representation. **b** Differences in current generated with reporter/target binding. Reporter/target binding was saturated from 10 fM, and a linear regression analysis shows the LOD of the target to be 10 aM. Current measurements (**a**) were performed using Keithley 6487 with a linear sweep 0–2 V at the step of 0.1 V. IDE, interdigitated electrode; LOD, limit of detection.

of differences in changes in current at each target DNA concentration, illustrating that a difference in current can be detected with as little as 10 fM, and that saturation was achieved at the concentration of 100 fM. The figure inset shows the linear regression analysis of target sequence detection from 10 aM to 10 fM, with the LOD seen at 100 aM. LOD was considered at the lowest concentration of an analyte from the calibration line to the background signal (S/N = 3:1; LOD = standard deviation of the baseline + 3σ). The limit of quantification was found to be at the level of 1 fM.

BDNF Gene Target Detection by Capture-Target-Reporter Sandwich Assay on the IDE Surface

The sandwich assay utilizing the capture probe and reporter was done to enhance the detection of the BDNF gene target sequence. As we found that 10 fM was the lowest concentration at which current changes could be detected, this target concentration was chosen to improve the detection by sandwich assay with the reporter and capture probe. Reporter oligos at concentrations ranging from 10 aM to 1 pM were dropped individually onto the target (10 fM), and alterations in current were registered after the washing step. As shown in Figure 4a, the reporter elicited clear increments in current at all concentrations tested. At a target concentration of 10 aM, the current level was 3.26E–07 A; however, the current level increased to 4.68E–07 A after interaction with 10 aM of the reporter. Moreover, when the reporter concentrations are enhanced to 100 aM, 1 fM, 10 fM, 100 fM, and 1 pM, the current levels are also gradually enhanced to 7.54E–07, 9.78E–07, 2.26E–06, 2.59E–06, and 2.71E–06 A, respectively. The 10 fM, 100 fM, and 1 pM reporter concentrations did not elicit any significant differences in current levels, indicating that the saturation point for target/reporter base-pairing had been achieved. This clear increment in current improves the target detection from 10 aM. There are other factors involved in the duplex formation, and it is not 100% to fulfill the ratio of 1:1. Especially, the biomolecular alignment and orientation play a crucial role. These possibilities make the linearity with the enhancement of the current level from 10 aM to 10 fM. Figure 4b depicts the changes in current interaction between the reporter (10 aM to 1 pM) and the target (10 aM), clearly showing the changes in current from a 10 aM concentration of the reporter and saturation at 10 fM. Linear regression analysis showed an LOD at 10 aM for reporter/target base-pairing. BDNF expressions are highly related to various psychiatric disorders, including anxiety, depression, and bipolar disorder [43]. Varying expressions of BDNF are also associated with different neuropsychiatric and neurodegenerative disorders, including Parkinson's, Huntington's, and Alzheimer's diseases [44]. Inset in Figure 4b shows a standard curve with the linear operating range of the device. Usually, the average range of BDNF polymorphisms falls in

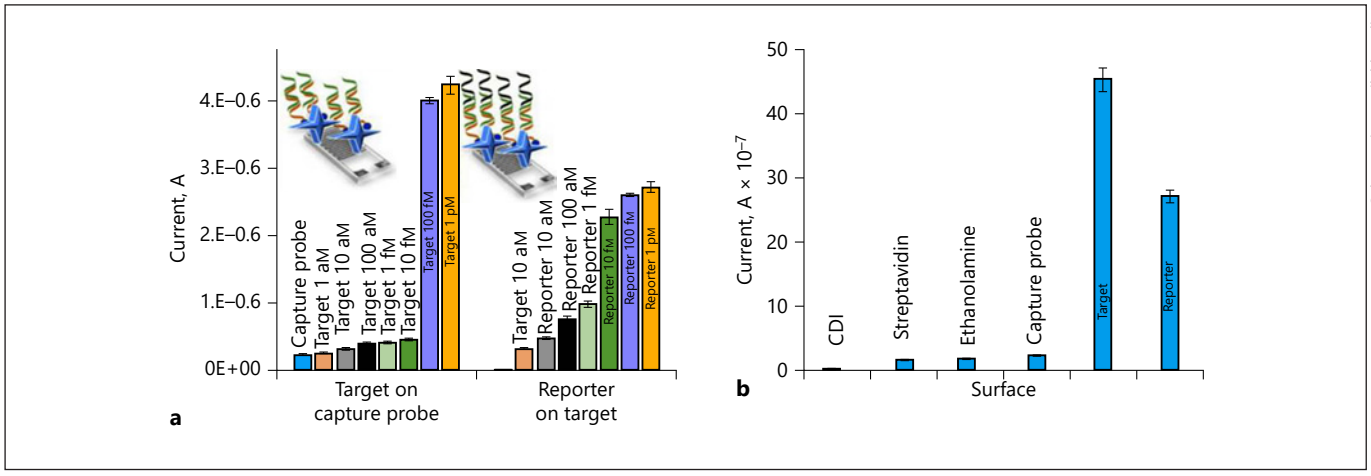

Fig. 5. a Comparison of changes in the current generated by target base-pairing with the capture probe and reporter. Target DNA binds to the capture probe from a concentration of 10 aM, and 10 aM of target detection was enhanced by the reporter. **Inset** A diagrammatic representation. **b** Reproducibility of the immobilization of each biomolecule on the IDE sensing surface. Current measurements (**a**) were performed using Keithley 6487 with a linear sweep 0–2 V at the step of 0.1 V. IDE, interdigitated electrode.

the range of 18–26 ng/mL for a normal adult, which is equivalent to 2.3–3.2 μM. The BDNF polymorphism mentioned is on the protein expression; however, it is hard to measure at the gene level. Furthermore, the expression of BDNF is decreasing in the nigrostriatal pathway and reflects the occurrence of neurogenerative diseases, such as Parkinson's disease. Validation of BDNF in the current study aids to develop a therapeutic agent for the neurogenerative disease [45]. The current work is determined in the range from low femtomolar till high picomolar, which indicates the higher reliability to be applied for covering the normal physiological relevant condition of patients. Figure 5a shows the overall comparison of current levels for target/capture probe binding and reporter/target binding. As can be seen, the capture probe from 10 aM of the target shows the increment of current; however, it is not significant. To enhance the detection, when the reporter was added, the current level was enhanced, providing evidence for detection of the target at 10 aM. These results indicate that the sandwich pattern with the capture probe-target-reporter enhanced the detection of the BDNF target gene.

The current study demonstrated the maximum reachable level to quantify the DNA expression at a lower abundance. It is possible to perform with biological samples, provided with samples extracted from the larger amount of cells as concentrated or by PCR-mediated amplification. Due to the large length of the gene sequence, it is hard to correlate the BDNF gene expression and the concentration of samples. The total genome of BDNF is 115,886 bp if considering only the BDNF genome in the extracted sample as 1 mg/mL. The final concentration would be 13 pM. However, it is not the case and always with other genomes and difficult to purify only the BDNF gene. Ultimately, the final concentration of BDNF is much lower.

Specific and Selective Detection of BDNF Target Gene

Figure 5b shows the reproducibility (average of triplicates) of detection with different surface modification steps carried out on the IDE surface. Here, apparently there is no obvious change in the ethanolamine blocking step, due to the very minimal available sites. A similar trend can be seen with the probe attachment due to the charge similarity to streptavidin. However, when attaching the single-strand DNA target, there is a dramatic enhancement in the charge that originates from the DNA phosphate backbone. With the reporter sequence complementation, the charge of phosphate molecules is getting masked, and there was a reverse change in the current trend. To attest to the selective determination of the BDNF gene sequence, 3 different control experiments were done with the capture probe immobilized on the modified IDE surface. Instead of target sequences, single- and triple-mismatched and noncomplementary sequences were reacted independently by the capture probe on the modified surfaces, and alterations in current were registered. Figure 6a shows the results of the control experiment for the target interaction with the capture probe, confirming that other control se-

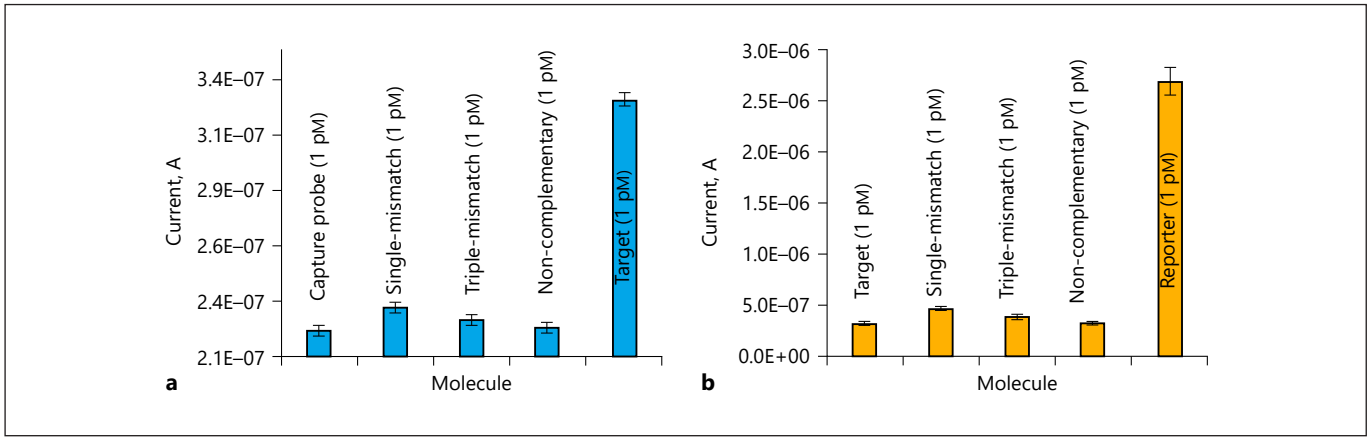

Fig. 6. Control experiments to confirm the selective detection of the BDNF gene sequence. Noncomplementary and single- and triple-mismatched sequences with the target (**a**) and reporter (**b**) were tested for control experimental analysis and compared with the detection of the perfect complement. The figure clearly shows that all the control experiments did not elicit significant changes in current when compared with the analysis using the specific sequence. Current measurements (**a**) were performed using Keithley 6487 with a linear sweep 0–2 V at the step of 0.1 V. BDNF, brain-derived neurotrophic factor.

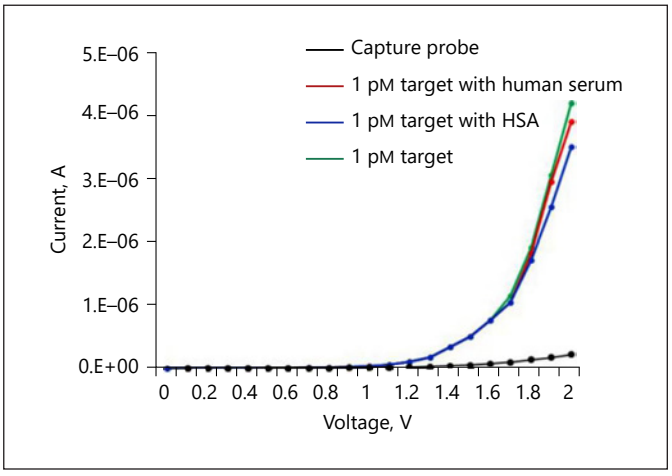

Fig. 7. Selectivity analysis: 1 pM of target was used by spiking into undiluted human serum and HSA (670 μM [45 mg/mL]). Higher specificity was found. HSA, human serum albumin.

quences do not elicit noticeable changes in current compared with those of the target. Figure 6b depicts the control experiment with single- and triple-mismatched and noncomplementary reporter sequences binding to the target, showing that these control sequences cannot significantly complement the target sequence, whereas the perfect base-pairing with the reporter sequence elicits clear increments in current levels. Both control experiments confirmed the selective binding of the BDNF target gene with capture and reporter sequences. After the control experiment, specific determination of the BDNF gene was done with the target sequence spiked in undiluted human serum or HSA. As shown in Figure 7, when 1 pM of the target sequence was placed, the current level was enhanced to 4.22E−06 A, while mixed with undiluted human serum and HSA (670 μM [45 mg/mL]) independently, they were 3.92E−06 and 4.02E−06 A, respectively. Not much difference was noticed, representing the specific determination of the target gene sequence for BDNF. Apart from this, generally, DNA strands are available in bodily fluids as double strands. To make them a single strand for the analysis, methods have been generated with the denaturation. The simpler strategy is denaturing the sample at 92°C for 1 or 2 min, which will linearize the DNA strands. The sensing surface was regenerated by using boiled water (92°C) and treated for 1 min 3 times. After 3 cycles, there was a reduction in the signal by 20%.

As displayed in this study, the primary advantage of aluminum microcomb electrodes on silicon wafer is with higher sensitivity and selectivity to finely discriminate the closely related DNA sequences by complementation. The overall sensing setup is suitable for both laboratory-based and point-of-care analyses, in addition, operating with alternate and direct current supplies. The fabricated sensing surface with gap and finger regions accommodates a wide range of biomolecular sizes from smaller to a whole cell with higher nonfouling. The sensing system shown here is with low cost, smaller in size, suitable for high-throughput analysis, and easier to operate. Considering the negative side, the sensing surface

is more opt for the oxide materials with appropriate surface chemistry, and when changes happen from metal oxides to other material, further optimization is needed. Apart from that, when minimizing the gap regions at the lower nanoscale level, the system tends to give a short circuit.

Conclusion

BDNF is from the neurotrophin growth factor family and participates in neuronal growth and survival. Dysregulation of BDNF expression is close to several disorders, such as bipolar disorder, depression, and Alzheimer's and Parkinson's diseases. Identifying and quantifying BDNF will aid in the provision of suitable treatments for affected patients. In this study, a target BDNF gene sequence was detected via a capture probe attached to an IDE surface, where the LOD was found to be 100 aM. To improve the detection, a sandwich assay for capture-target-reporter was done on the IDE sensing surface. We found that the reporter sequence at concentrations ranging from 10 aM to 1 pM elicited incremental alterations in current for the determination of 10 aM target DNA. Control experiments with single- and triple-mismatch and noncomplementary sequences did not elicit significant alterations in the current, indicating the selective detection of the BDNF gene sequence. This experimental setup will aid in the quantification of BDNF and improve treatment for patients presenting with BDNF-related disorders.

Statement of Ethics

All procedures performed in study were in accordance with the ethical standards of the institutional and/or national research committee and with the 1964 Helsinki Declaration and its later amendments or comparable ethical standards.

Conflict of Interest Statement

The authors declare that they have no competing interests.

Funding Sources

No funding was received.

Author Contributions

Z.L. and L.C. conceptualized and designed the study, H.Z. and J.D. analyzed data and drafted the manuscript, S.G. and T.L. collected the data and helped in data analysis, and X.X. performed proof reading and final editing along with the guarantor of the manuscript.

References

1 Goda A, Ohgi S, Kinpara K, Shigemori K, Fukuda K, Schneider EB. Changes in serum BDNF levels associated with moderate-intensity exercise in healthy young Japanese men. Springerplus. 2013;2:678.
2 Cohen-Cory S, Kidane AH, Shirkey NJ, Marshak S. Brain-derived neurotrophic factor and the development of structural neuronal connectivity. Dev Neurobiol. 2010;70(5):271–88.
3 Liu C, Jiao C, Wang K, Yuan N. DNA methylation and psychiatric disorders. Prog Mol Biol Transl Sci. 2018;157:175–232.
4 Hachisu M, Konishi K, Hosoi M, Tani M, Tomioka H, Inamoto A, et al. Beyond the hypothesis of serum anticholinergic activity in Alzheimer's disease: acetylcholine neuronal activity modulates brain-derived neurotrophic factor production and inflammation in the brain. Neurodegener Dis. 2015;15:182–87.
5 Licznerski P, Jonas EA. BDNF signaling: harnessing stress to battle mood disorder. Proc Natl Acad Sci U S A. 2018;115(15):3742–4.
6 Akhtar MH, Hussain KK, Gurudatt NG, Chandra P, Shim YB. Ultrasensitive dual probe immunosensor for the monitoring of nicotine induced-brain derived neurotrophic factor released from cancer cells. Biosens Bioelectron. 2018;116:108–15.
7 Bockaj M, Fung B, Tsoulis M, Foster WG, Soleymani L. Method for electrochemical detection of brain derived neurotrophic factor (BDNF) in plasma. Anal Chem. 2018;90(14):8561–6.
8 Giannini A, Bucci F, Luisi S, Cela V, Pluchino N, Merlini S, et al. Brain-derived neurotrophic factor in plasma of women with endometriosis. J Endometr. 2010;2(3):144–50.
9 Aparna Sharma AH. Serum BDNF: a potential biomarker for major depressive disorder and antidepressant response prediction. J Depress Anxiety. 2015;4(2):55967667.
10 Park CH, Kim J, Namgung E, Lee D-W, Kim GH, Kim M, et al. The BDNF val66met polymorphism affects the vulnerability of the brain structural network. Front Hum Neurosci. 2017;11:400.
11 Chen ZY, Jing D, Bath KG, Ieraci A, Khan T, Siao C-J, et al. Genetic variant BDNF (Val66Met) polymorphism alters anxiety-related behavior. Science. 2006;314(5796):140–3.
12 Sánchez-Romero MA, Dorado P, Guarino E, Llerena A. Development of a new genotyping assay for detection of the BDNF Val66Met polymorphism using melting-curve analysis. Pharmacogenomics. 2009;10(6):989–95.
13 Naegelin Y, Dingsdale H, Säuberli K, Schädelin S, Kappos L, Barde Y-A. Measuring and validating the levels of brain-derived neurotrophic factor in human serum. eNeuro. 2018;5(2):ENEURO.0419-17.2018.
14 Polacchini A, Metelli G, Francavilla R, Baj G, Florean M, Mascaretti LG, et al. A method for reproducible measurements of serum BDNF: comparison of the performance of six commercial assays. Sci Rep. 2015;5:17989.
15 Gopinath SC, Tang TH, Citartan M, Chen Y, Lakshmipriya T. Current aspects in immunosensors. Biosens Bioelectron. 2014;57:292–302.

16 Wang C, Lakshmipriya T, Gopinath SCB. Amine-aldehyde chemical conjugation on a potassium hydroxide-treated polystyrene ELISA surface for nanosensing an HIV-p24 antigen. Nanoscale Res Lett. 2019;14(1):21.
17 Gopinath SCB, Awazu K, Fujimaki M. Detection of influenza viruses by a waveguide-mode sensor. Anal Methods. 2010;2(12):1880.
18 Gopinath SC, Hayashi K, Lee JB, Kamori A, Dong CX, Hayashi T, et al. Analysis of compounds that interfere with herpes simplex virus-host receptor interactions using surface plasmon resonance. Anal Chem. 2013;85(21):10455–62.
19 Cosnier S. Electrochemical biosensors; 2014.
20 Letchumanan I, Md Arshad MK, Balakrishnan SR, Gopinath SCB. Gold-nanorod enhances dielectric voltammetry detection of c-reactive protein: a predictive strategy for cardiac failure. Biosens Bioelectron. 2019;130:40–7.
21 Sadat Mousavi P, Smith SJ, Chen JB, Karlikow M, Tinafar A, Robinson C, et al. A multiplexed, electrochemical interface for gene-circuit-based sensors. Nat Chem. 2020;12(1):48–55.
22 Tan EKW, Au YZ, Moghaddam GK, Occhipinti LG, Lowe CR. Towards closed-loop integration of point-of-care technologies. Trends Biotechnol. 2019;37(7):775–88.
23 Grieshaber D, MacKenzie R, Vörös J, Reimhult E. Electrochemical biosensors: sensor principles and architectures. Sensors. 2008;8(3):1400–58.
24 Kang X, Wang J, Wu H, Liu J, Aksay IA, Lin Y. A graphene-based electrochemical sensor for sensitive detection of paracetamol. Talanta. 2010;81(3):754–9.
25 Swamy BE, Venton BJ. Subsecond detection of physiological adenosine concentrations using fast-scan cyclic voltammetry. Anal Chem. 2007;79(2):744.
26 Yang W, Lai RY. Comparison of the stem-loop and linear probe-based electrochemical DNA sensors by alternating current voltammetry and cyclic voltammetry. Langmuir. 2011;27(23):14669.
27 Tang X, Bansaruntip S, Nakayama N, Yenilmez E, Chang YL, Wang Q. Carbon nanotube DNA sensor and sensing mechanism. Nano Lett. 2006;6(8):1632.
28 Dai W, Sheikh MA, Milenkovic O, Baraniuk RG. Compressive sensing DNA microarrays. EURASIP J Bioinform Syst Biol. 2009;2009(1):162824.
29 Diculescu V, Paquim A-M, Brett AM. Electrochemical DNA sensors for detection of DNA damage. Sensors. 2005;5(6):377–93.
30 Jacobs CB, Peairs MJ, Venton BJ. Review: carbon nanotube based electrochemical sensors for biomolecules. Anal Chim Acta. 2010;662(2):105.
31 Xiao Y, Lai RY, Plaxco KW. Preparation of electrode-immobilized, redox-modified oligonucleotides for electrochemical DNA and aptamer-based sensing. Nat Protoc. 2007;2(11):2875.
32 Wang J. Electrochemical biosensors: towards point-of-care cancer diagnostics. Biosens Bioelectron. 2006;21(10):1887.
33 Xu W, Jin T, Dai Y, Liu CC. Surpassing the detection limit and accuracy of the electrochemical DNA sensor through the application of CRISPR Cas systems. Biosens Bioelectron. 2020;155(5):112100.
34 Chen S, Sun Y, Xia Y, Lv K, Man B, Yang C. Donor effect dominated molybdenum disulfide/graphene nanostructure-based field-effect transistor for ultrasensitive DNA detection. Biosens Bioelectron. 2020;156(5):112128.
35 Hwang MT, Heiranian M, Kim Y, You S, Leem J, Taqieddin A, et al. Ultrasensitive detection of nucleic acids using deformed graphene channel field effect biosensors. Nat Commun. 2020;11(1):1543.
36 Letchumanan I, Gopinath SCB, Md Arshad MK, Anbu P, Lakshmipriya T. Gold nano-urchin integrated label-free amperometric aptasensing human blood clotting factor IX: a prognosticative approach for 'Royal disease. Biosens Bioelectron. 2019;131:128–35.
37 Ramanathan S, Gopinath SCB, Md Arshad MK, Poopalan P, Loong FK, Lakshmipriya T, et al. Assorted micro-scale interdigitated aluminium electrode fabrication for insensitive electrolyte evaluation: zeolite nanoparticle-mediated micro- to nano-scaled electrodes. Appl Phys A. 2019;125(8):548.
38 Gopinath SC, Awazu K, Fujimaki M, Shimizu K, Mizutani W, Tsukagoshi K. Surface functionalization chemistries on highly sensitive silica-based sensor chips. Analyst. 2012;137(15):3520.
39 Zheng S, Zhang H, Lakshmipriya T, Gopinath SCB, Yang N. Gold nanorod integrated electrochemical sensing for hyperglycaemia on interdigitated electrode. Biomed Res Int. 2019;2019:9726967.
40 Lakshmipriya T, Gopinath SC, Tang TH. Biotin-streptavidin competition mediates sensitive detection of biomolecules in enzyme linked immunosorbent assay. PLoS One. 2016;11(3):e0151153.
41 Lakshmipriya T, Horiguchi Y, Nagasaki Y. Co-immobilized poly(ethylene glycol)-block-polyamines promote sensitivity and restrict biofouling on gold sensor surface for detecting factor IX in human plasma. Analyst. 2014;139(16):3977–85.
42 Nagasaki Y, Kobayashi H, Katsuyama Y, Jomura T, Sakura T. Enhanced immunoresponse of antibody/mixed-PEG co-immobilized surface construction of high-performance immunomagnetic ELISA system. J Colloid Interface Sci. 2007;309(2):524–30.
43 Yoo YK, Lee J, Kim J, Kim G, Kim S, Kim J, et al. Ultra-sensitive detection of brain-derived neurotrophic factor (BDNF) in the brain of freely moving mice using an interdigitated microelectrode (IME) biosensor. Sci Rep. 2016;6:33694.
44 Karege F, Perret G, Bondolfi G, Schwald M, Bertschy G, Aubry JM. Decreased serum brain-derived neurotrophic factor levels in major depressed patients. Psychiatry Res. 2002;109(2):143.
45 Palasz E, Wysocka A, Gasiorowska A, Chalimoniuk M, Niewiadomski W, Niewiadomska G. BDNF as a promising therapeutic agent in parkinson's disease. Int J Mol Sci. 2020;21(3):1170.
46 Robinson RC, Radziejewski C, Spraggon G, Greenwald J, Kostura MR, Burtnick LD, et al. The structures of the neurotrophin 4 homodimer and the brain-derived neurotrophic factor/neurotrophin 4 heterodimer reveal a common Trk-binding site. Protein Sci. 1999;8(12):2589.